University of Groningen

Hyperinsulinemia Adversely Affects Lung Structure and Function

Singh, Suchita; Bodas, Manish; Bhatraju, Naveen Kumar; Pattnaik, Bijay; Gheware, Atish; Kolumam Parameswaran, Praveen; Thompson, Michael A; Freeman, Michelle; Mabalirajan, Ulaganathan; Gosens, Reinoud

IMPORTANT NOTE: You are advised to consult the publisher's version (publisher's PDF) if you wish to cite from it. Please check the document version below.

Document Version
Publisher's PDF, also known as Version of record

Publication date:
2016

Link to publication in University of Groningen/UMCG research database

Hyperinsulinemia adversely affects lung structure and function

Suchita Singh,[1]* Manish Bodas,[1]* Naveen K. Bhatraju,[1] Bijay Pattnaik,[1] Atish Gheware,[1]
Praveen Kolumam Parameswaran,[5] Michael Thompson,[5] Michelle Freeman,[5] Ulaganathan Mabalirajan,[1]
Reinoud Gosens,[6] Balaram Ghosh,[1] Christina Pabelick,[5] Allan Linneberg,[2,3,4] Y. S. Prakash,[5]
and Anurag Agrawal[1]

[1]*Center of Excellence for Translational Research in Asthma and Lung Disease, CSIR-Institute of Genomics and Integrative Biology,
New Delhi, India;* [2]*Research Centre for Prevention and Health, the Capital Region of Denmark, Copenhagen, Denmark;*
[3]*Department of Clinical Experimental Research, Glostrup University Hospital, Glostrup, Denmark;* [4]*Department of Clinical
Medicine, Faculty of Health and Medical Sciences, University of Copenhagen, Copenhagen, Denmark;* [5]*Departments of
Anesthesiology and Physiology and Biomedical Engineering, Mayo Clinic, Rochester, Minnesota; and* [6]*Department of Molecular
Pharmacology, Groningen Research Institute for Asthma and COPD (GRIAC), University of Groningen, Groningen, Netherlands*

Singh S, Bodas M, Bhatraju NK, Pattnaik B, Gheware A,
Parameswaran PK, Thompson M, Freeman M, Mabalirajan U,
Gosens R, Ghosh B, Pabelick C, Linneberg A, Prakash YS, Agrawal
A. Hyperinsulinemia adversely affects lung structure and function. *Am J
Physiol Lung Cell Mol Physiol* 310: L837–L845, 2016. First published
February 26, 2016; doi:10.1152/ajplung.00091.2015.—There is limited
knowledge regarding the consequences of hyperinsulinemia on the
lung. Given the increasing prevalence of obesity, insulin resistance,
and epidemiological associations with asthma, this is a critical lacuna,
more so with inhaled insulin on the horizon. Here, we demonstrate
that insulin can adversely affect respiratory health. Insulin treatment
(1 µg/ml) significantly ($P < 0.05$) increased the proliferation of
primary human airway smooth muscle (ASM) cells and induced
collagen release. Additionally, ASM cells showed a significant in-
crease in calcium response and mitochondrial respiration upon insulin
exposure. Mice administered intranasal insulin showed increased
collagen deposition in the lungs as well as a significant increase in
airway hyperresponsiveness. PI3K/Akt mediated activation of
β-catenin, a positive regulator of epithelial-mesenchymal transition
and fibrosis, was observed in the lungs of insulin-treated mice and
lung cells. Our data suggests that hyperinsulinemia may have adverse
effects on airway structure and function. Insulin-induced activation of
β-catenin in lung tissue and the contractile effects on ASM cells may
be causally related to the development of asthma-like phenotype.

insulin resistance; hyperinsulinemia; lung function; β-catenin

OBESITY, DIABETES, AND ASTHMA have attained global epidemic
proportions (19, 20). Multiple studies have shown a strong
epidemiological and experimental link between obesity and
asthma that further relates to a diverse set of etiologic factors
including altered lung mechanics, adipose hormones, and in-
flammatory cytokines (3, 11). Although a positive relationship
between diabetes and asthma is less certain (36, 37), there is
strong evidence that overt diabetes and its precursor form of
insulin resistance are strongly associated with reduced lung
function characterized by low forced expiratory volume in 1 s
(FEV_1) and forced vital capacity (FVC) while maintaining a
normal ratio (6, 21, 25, 33). Such restrictive low lung function
is not infrequent in population studies, ~10% or more (16).
Perhaps more interestingly, it is linked to an increased risk of
future obstructive lung disease as well as components and risks
of the metabolic syndrome, namely continued insulin resis-
tance, diabetes, hypertension, atherosclerosis, and cardiac
events, among others (14, 16, 23, 25, 29, 39). For asthma, a
strong positive association between insulin resistance and
asthma, independent of adiposity, has been reported by some
studies, but this has not been consistently observed in other
studies (8, 17, 24). Hence, it is not clear whether insulin
resistance, with consequent hyperinsulinemia, is a dependent
surrogate marker or whether it independently contributes to
increased risk of respiratory disease. Furthermore, although
there is sufficient basis to hypothesize that hyperinsulinemia is
mechanistically related to increased risk of asthma or other
lung diseases, there are only limited data to support this idea,
with insulin showing potentiation of airway smooth muscle
(ASM) contraction in animals (15, 32), which remains to be
confirmed in human airways (34). Indeed, the mechanisms by
which insulin influences airway elements to produce structural
and functional changes in the asthmatic airway are also not
known.

Understanding the impact of hyperinsulinemia on lung
health is a critical issue not just from a research perspective,
but also as a global healthcare issue, given that insulin resis-
tance is on the rise worldwide. The increasing interest in
clinical use of inhaled insulin formulations that could lead to
very high levels of insulin in the lung also illustrates the need
for focused studies on insulin and lung health, given that there
have been reports of negative effects on lung function with a
previous formulation, Exubera (Pfizer) (5).

To investigate possible mechanisms of such associations and
the potential causal effects of high lung levels of insulin, in
vitro human lung cell models with insulin application and
preclinical in vivo murine model of intranasal insulin applica-
tion were tested. Overall, these studies led to a better under-
standing of potentially deleterious insulin-induced signaling in
the lung.

MATERIALS AND METHODS

Murine Experiments

Male Balb/c mice (8–10 wk old) were obtained from National
Institute of Nutrition, Hyderabad, India and were acclimatized for
1 wk. All procedures were approved by CPCSEA (Committee for the
Purpose of Control and Supervision of Experiments on Animals),
CSIR-IGIB, Delhi, India.

---

* S. Singh and M. Bodas contributed equally to this work.
Address for reprint requests and other correspondence: A. Agrawal, Center
of Excellence for Translational Research in Asthma and Lung Disease,
CSIR-Institute of Genomics and Integrative Biology, New Delhi 110007, India
(e-mail: a.agrawal@igib.in).

Intranasal insulin-induced hyperinsulinemia model. The model was developed in Balb/c mice: 50 μg insulin was administered intranasally, daily for 11 days. Mice were euthanized on the 12th day, by overdose of pentobarbital. The 50-μg intranasal dose was selected from pilot studies of 5–500 μg since it led to insulin levels of ~200 pmol/l, comparable to levels seen in insulin resistant humans.

Glucose tolerance test. After 11 days of insulin treatment as described above, the mice were kept fasting for 6 h and a oral glucose
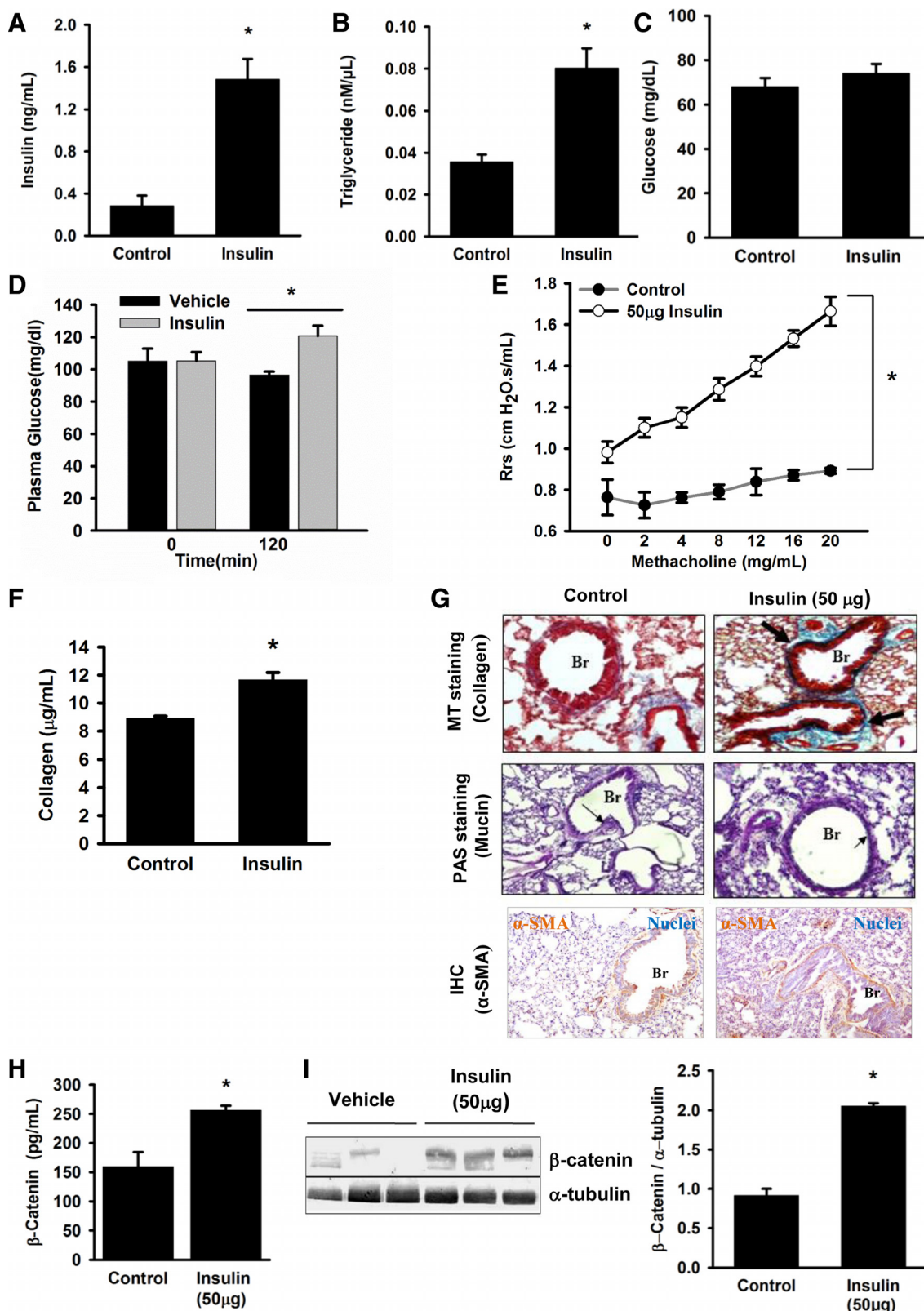
load (1 g/kg body wt) was delivered into the stomach by a 20-gauge gavage needle. The blood glucose was measured via a commercially available glucometer with tail vein blood at 0 and 120 min.

β-Catenin knockdown in mice lungs. Mice were treated with four doses of β-catenin siRNA (Sigma), 75 μg, alongside of intranasal insulin treatment every 48 h starting from the 4th day and continued till the end of the hyperinsulinemia model. Mice were euthanized on 12th day as described above.

Measurement of AHR. Airway hyperresponsiveness (AHR) measurements were done after 11 days. Mice were anesthetized with intraperitoneal 16 mg/kg xylazine and 50 mg/kg pentobarbital and surgically prepared with a tracheal cannula (18 gauge). Lung function measurements were performed in anesthetized and paralyzed mice, and respiratory system parameters (airway resistance; R) were measured with a flexiVent system (SCIREQ). The methacholine nebulization was performed by using the default protocol of system software (SCIREQ) with standard particle-sized model nebulizer (4–6 μM particle size) with 10-s nebulization time, 50% duty cycle, presence of attached Drierite tube (desiccant), and regular ventilation profile. The respiratory system resistance had been shown as R or Rrs with its unit ($cmH_2O \cdot s \cdot ml^{-1}$).

Histology. Histological staining was performed in paraffin-embedded lung sections by standard protocols (4).

Measurement of collagen content. Mice lungs were homogenized in RIPA buffer supplemented with DTT (1 mM) and protease inhibitor cocktail (Sigma). Collagen content in the total lung homogenate was determined by using the Sircol Collagen Assay kit (Biocolor, Carrickfergus, UK) as per manufacturer's instructions and results were represented as relative fluorescence units per microgram lung protein.

Immunohistochemistry. Formalin-fixed, paraffin-embedded lung tissue sections were prepared for immunohistochemical analysis. Sections were stained with the primary antibodies for α-smooth muscle actin (rabbit polyclonal antibody; Abcam) followed by horseradish peroxidase (HRP)-conjugated secondary antibodies (Bang Genei). The signal was detected by diaminobenzidine tetrahydrochloride (DAB, Sigma), and hematoxylin was used as a counterstain.

Cell Culture

BEAS-2B (human bronchial epithelial cells) were directly purchased from either ECACC or ATCC and maintained under standard cell culture conditions as described by ECACC or ATCC.

Isolation of human ASM cells. Human ASM were isolated from surgical lung samples as previously described (31).

Insulin treatment. Following serum starvation, ASM cells were plated in 60-mm sterile tissue culture dishes or T75 flasks and treated with different concentrations of recombinant human insulin (Sigma) for the indicated time points. For other experiments, ASM cells were either plated in 96-well plates [extracellular matrix (ECM), proliferation, or Ca^{2+} assays] or on special 24-well plates provided by Seahorse Biosciences (for mitochondrial function assays).

Cell proliferation. ASM cells and BEAS-2B cells were plated at a concentration of 5,000 cells/well and serum starved for 16 h prior to

treatment. The plates were then treated with insulin (1 μg/ml), β-catenin inhibitor (ICG-001, SelleckChem) at 1 μM concentration, and combination of insulin and β-catenin inhibitor in 1% serum-containing medium. Readouts for cell proliferation were taken after 72 h by using the MTS assay kit from Promega at 490 nm.

Immunofluorescence protocol. ASM and BEAS-2B cells were plated at a concentration of 10,000 cells/ml. Cells were serum starved and treated with 1 μg/ml insulin for 1 h prior to fixation with 4% paraformaldehyde. Cell were permeabilized with 0.1% Triton for 20 min and blocked with 4% BSA. β-Catenin primary antibody was used at 100 μg/ml (ab16051, Abcam) in 4% BSA and 1 mg/ml Alexa Fluor 488 secondary antibody (A21208, Life Technologies) and imaged at 490 nm in a fluorescent microscope.

Western blotting. Total or cytosolic extracts were prepared from cells treated with insulin (1 μg/ml) alone or with wortmannin (1 μM, pretreatment for 1 h), and from lung tissue of mice administered intranasal insulin (50 μg/ml), by standard procedures. Protein estimation was done by the BCA method, and equal amounts of protein were resolved on SDS-PAGE, followed by transfer onto PVDF/nitrocellulose membrane (Millipore). The membranes were incubated with primary antibodies against pAkt, Akt, IR-1β, activated IR-1β, pGSK3β, GSK3-β, β-catenin, α-tubulin, and GAPDH (Santa Cruz Biotechnology, Abcam, or Cell Signaling). Proteins were detected by using Li-Cor IR Dye secondary antibodies and imaged on the Li-Cor Odyssey. Alternatively, HRP-conjugated secondary antibody (Sigma) with DAB (3,3′-diaminobenzidine tetrahydrochloride) chromogen was used.

ECM deposition assay. ASM cells were serum starved and incubated with different doses of insulin for 72 h. Cells were washed in PBS and 100 μl of 0.016 N NH_4OH was added to lyse the cells, thus leaving only the native deposited ECM on the well surface. Wells were washed with PBS again and incubated with 5% BSA (in PBS) or Li-Cor blocking buffer for 90 min and then incubated in 1:100 dilution of collagen-1 primary antibody (Abcam, rabbit polyclonal) for 2 h at room temperature (RT) or overnight at 4°C. Plates were washed again with 0.1% Tween 20 in PBS and then incubated with appropriate secondary antibody (Licor IRDye donkey anti-rabbit 800 CW) for 1 h at RT. After a final wash, the extent of collagen deposition was assessed by a Licor Odyssey system. Wells without any cells were used as background controls.

Ca^{2+} assay. ASM cells were serum deprived and incubated in 5 μM fluo-4/AM (no. F14217, Invitrogen; excitation 495 nm; emission 510 nm) for 60 min at RT, followed by insulin (1 μg/ml) treatment for 30 min. Baseline intracellular calcium ($[Ca^{2+}]_i$) levels were assessed by use of a fluorescence imaging plate reader (FlexStation 3, Molecular Devices, Sunnyvale, CA). Fluo-4 levels were converted to nanomolar Ca^{2+} by previously described empirical calibration procedures (1).

Seahorse experiments. Human ASM cells were seeded into a 24-well XF24 plate and serum starved for 24 h. Cells were then treated with 1 μg/ml insulin overnight (~16 h). Prior to assay cells were equilibrated in Seahorse assay medium containing 10 mM glucose at 37°C for 1 h. Mitochondrial function was determined via a

---

Fig. 1. Intranasal insulin treatment caused hyperinsulinemia, impaired glucose tolerance, and asthma-like features in mice. Mice were intranasally administered with insulin (50 μg) or vehicle [0.01 N hydrochloric acid (HCl)] for 11 days and were euthanized on day 12 after overnight fasting. Serum samples from control and insulin-treated groups were analyzed for insulin (*A*), triglycerides (*B*), and fasting glucose levels (*C*). Glucose tolerance was measured by comparing the blood glucose levels of vehicle- and insulin-treated mice groups, after 2 h of oral glucose (25 mg) administration. The time 0 min indicates the baseline glucose levels (*D*). To assess the effect of insulin on lung structure and function a series of parameters have been measured: change in respiratory system resistance (Rrs) to nonspecific bronchoconstrictor, methacholine (*E*), and collagen levels in total lung lysate, as measured by Sircol assay (*F*). Representative images of Masson's trichrome (MT) staining (*top*), periodic acid Schiff (PAS) staining (*middle*), immunohistochemistry (IHC) for α-smooth muscle actin (α-SMA) (*bottom*) used to measure subepithelial fibrosis, mucus metaplasia and smooth muscle mass, respectively (*G*). β-Catenin levels were measured, by ELISA, in total lung lysate of both insulin- and vehicle-treated mice (*H*). The result from (*H*) was corroborated by immunoblotting of β-catenin in total lung lysate of both insulin- and vehicle-treated mice (*I*). Magnification ×10 (MT and PAS staining), ×20 (IHC); scale 20 μm. Data represent means ± SE, n = 4–6, *P ≤ 0.05, compared with control. Br, Bronchi; Rrs, airway resistance.

XF Cell Mito Stress Test assay following standard protocols determined by Seahorse Biosciences. Oxygen consumption rate (OCR) and hydrogen production (ECAR) were measured in real time with fluorescent probes. OCR/ECAR measurements were taken every 5 min in the following sequence: four measurements for baseline, four measurements after addition of 9 μM oligomycin, four measurements after addition of

0.3 μM FCCP (carbonyl cyanide *p*-trifluoromethoxyphenylhydrazone), and four measurements following the addition of 11 μM antimycin A and 11 μM rotenone. OCR/ECAR values were normalized to well protein concentration and expressed per microgram protein. Mitochondrial ATP production, maximal respiration, and spare capacity were derived from OCR measurements by using Seahorse Biosciences suggested formulae.
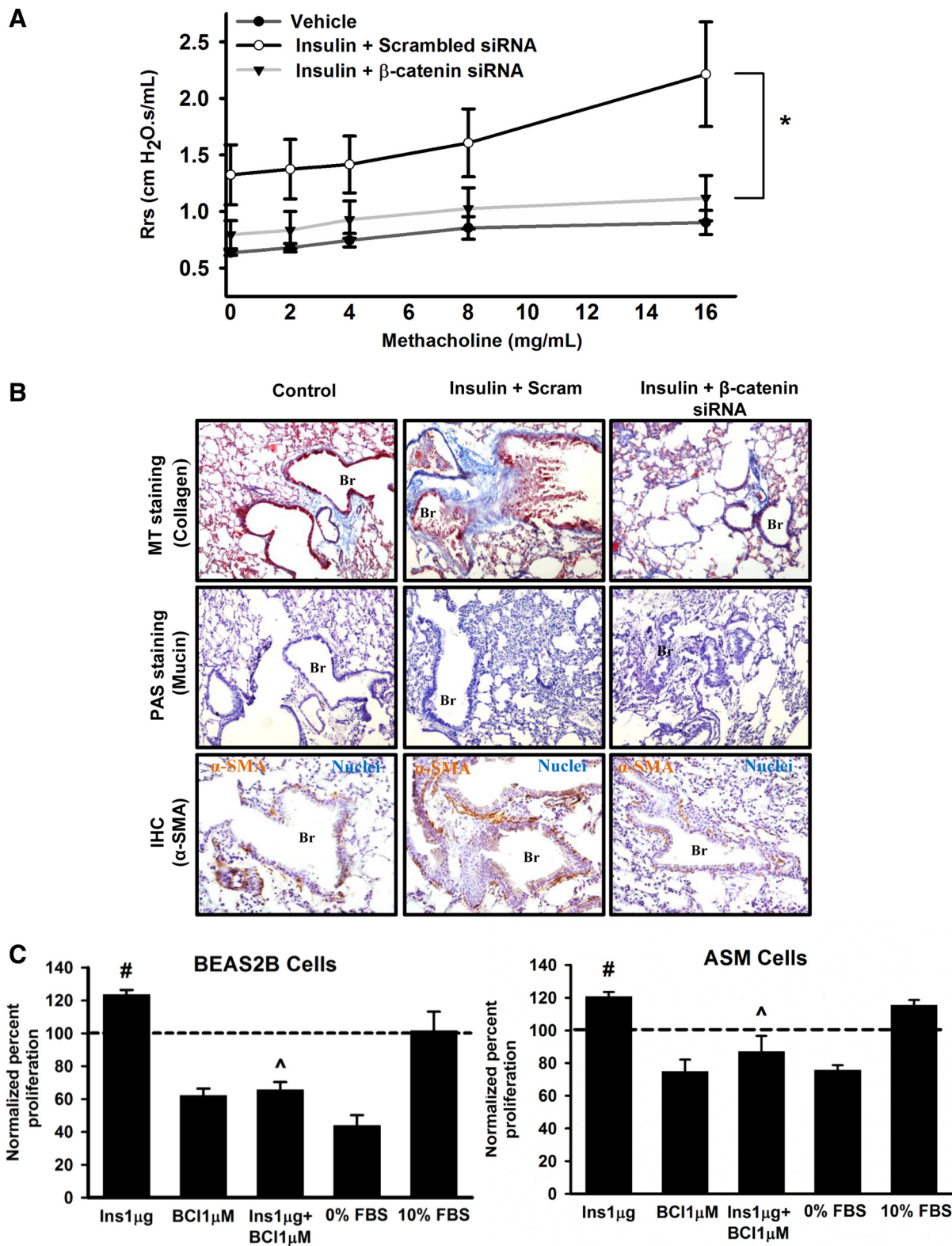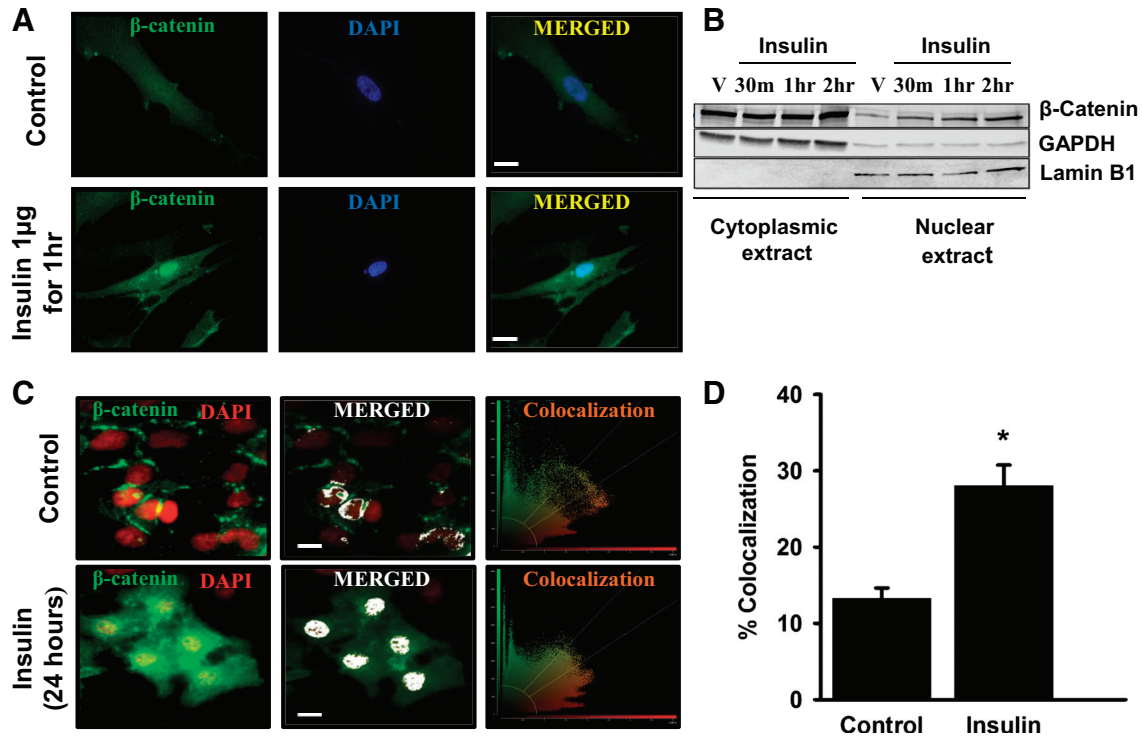
Fig. 3. Insulin induces β-catenin nuclear localization in ASM and BEAS2B cells. The effect of insulin on subcellular localization of β-catenin was investigated in both transformed human bronchial epithelial (BEAS2B) and primary human airway smooth muscle (ASM) cells. Insulin (1 μg)-induced β-catenin translocation to nucleus, in ASM cells, was confirmed by fluorescence imaging after 1 h (A) and immunoblotting of β-catenin in cytoplasmic and nuclear extracts before insulin treatment (V) and at different time points [30 min (30 m), 1 h, and 2 h] posttreatment (B). β-Catenin translocation to nucleus in BEAS2B cells was confirmed by measuring colocalization rates of fluorescent markers represented as green (β-catenin) and red (nucleus). *Left*, merged fluorescent image; *middle*, colocalized regions (white); *right*, scatterplot of the acquired image processed by the LAS AF software (Leica). The colocalization rate is the percentage of colocalization extent calculated from the ratio of the areas of colocalizing fluorescent markers and that of image foreground (C). Bar plot showing the mean colocalization rates corresponding to control and insulin-treated BEAS2B cells (D). Magnification ×63; scale 20 μm. Data represent means ± SE, $n = 6$, *$P \leq 0.05$, compared with respective controls. GAPDH, glyceraldehyde-3-phosphate dehydrogenase; V, vehicle.

Statistical analysis. Data are expressed as means ± SE. Significant differences between two groups were estimated by unpaired Student *t*-test. For experiments with more than two groups, data were analyzed by one-way ANOVA followed by Tukey post hoc testing. Statistical significance was set at *$P \leq 0.05$.

RESULTS

Intranasal Insulin Administration to Mice Induces Insulin Resistance, Increased Lung β-Catenin Levels, Collagen Deposition, and AHR

Repeated intranasal insulin administration, at a dose sufficient to increase circulating insulin to physiological hyperinsulinemic levels, was associated with insulin resistance as indicated by increased serum triglyceride levels and glucose intolerance (Fig. 1, *A–D*). This was further associated with increased AHR to methacholine challenge (Fig. 1*E*). Increased insulin levels also led to a significant increase in lung collagen levels (Fig. 1*F*). Histological analysis of lung sections of these mice shows increased peribronchial collagen deposition (Fig. 1*G, top*), without a significant increase in mucin content (Fig. 1*G, middle*). Furthermore, immunohistochemistry for α-smooth muscle actin (α-SMA) in the insulin-treated mice showed a significant increase in its levels suggesting an increase in proliferation of smooth muscle cells (Fig. 1*G, bottom*). Taken together, the data indicate that hyperinsulinemia induces asthma-like pathophysiological features. β-Catenin, a known mediator of smooth muscle cell proliferation, has been reported to be induced by insulin. To

Fig. 2. Inhibition of β-catenin attenuates asthma-like features and smooth muscle cell proliferation. Mice were treated, intranasally, with insulin (50 μg) or vehicle (0.01 N HCl) for 11 consecutive days. The insulin-treated mice were administered with 4 intratracheal doses of either scrambled siRNA (Scram; 75 μg/mice) or β-catenin siRNA (75 μg/mice) on alternative days starting from the 4th day of insulin treatment. The effect of β-catenin knockdown on lung function was determined by measuring airway responsiveness to nonspecific bronchoconstrictor methacholine (*A*). Formalin-fixed, paraffin-embedded lung sections were analyzed by MT staining (*top*), PAS staining (*middle*), and IHC of α-smooth muscle actin (α-SMA) (*bottom*) for lung structural features subepithelial fibrosis, mucus metaplasia, and smooth muscle mass, respectively (*B*). Cell proliferation rates were measured in vitro, for transformed human bronchial epithelial (BEAS2B) cells and primary human airway smooth muscle (ASM) cells, in the presence of insulin (Ins; 1 μg) and/or β-catenin inhibitor (BCI) (1 μM). Untreated cells maintained in culture medium containing 0% fetal bovine serum (FBS) and 10% FBS correspond to the negative and positive control, respectively (*C*). All the data are represented as normalized percentages of the absorbance values obtained for untreated cells maintained in culture medium with 1% FBS (control; represented as dotted line in the plot). Data represent means ± SE, $n = 3–5$. *$P \leq 0.05$, compared with insulin + scrambled siRNA-treated group. #$P \leq 0.05$, compared with control. ^$P < 0.05$, compared with insulin-treated condition. Br, Bronchi; Ins, Insulin.

investigate whether β-catenin is involved in the aforementioned insulin-mediated effects, we measured β-catenin level in total lung protein. A significant increase in lung β-catenin level was observed in hyperinsulinemic mice (Fig. 1, *H*, ELISA and *I*, Western blot).

β-Catenin Is Causally Associated with the Insulin-Induced Altered Lung Function in Mice

To establish the causal role of β-catenin in insulin-induced asthma-like features, we investigated the effects of β-catenin knockdown on the lung structure and function of hyperinsulinemic mice. We found a significant decrease in the airway responsiveness to methacholine challenge, in insulin+β-catenin siRNA-treated mice, compared with mice treated with insulin+scrambled siRNA (Fig. 2*A*). This observation was further corroborated by less peribronchial collagen deposition (Fig. 2*B*, *top*) and decreased smooth muscle actin (Fig. 2*B*, *bottom*) in lung sections of insulin and β-catenin siRNA-treated mice, compared with mice treated with similar doses of insulin and scrambled siRNA. To gain a better mechanistic understanding of how intranasal insulin administration induced asthma-like features, we also investigated the effects of insulin

on cultured cells. Insulin treatment induced a proliferative phenotype in human ASM cells in vitro in a β-catenin-dependent manner (Fig. 2*C*, *right*). Treatment with a β-catenin inhibitor, alone or in combination with insulin, resulted in a significant reduction of ASM cell proliferation, compared with vehicle control and cells treated with insulin, respectively (Fig. 2*C*, *right*). Figure 2*C*, *left*, shows the proliferative effects of insulin and the antiproliferative effects of β-catenin inhibition in BEAS-2B cells in vitro. Freshly isolated primary epithelial cells from human lung tissue also showed increased proliferation with identical insulin treatment, with proliferating cell nuclear antigen being increased by ~20%. In view of identical effects between the primary cells and BEAS-2B cell line, BEAS-2B cells were used for further studies of mechanisms by which β-catenin was upregulated.

β-Catenin Activation and Nuclear Translocation Is Via the PI3-Akt-GSK3β Pathway

Proliferative effects of β-catenin are known to be dependent on its nuclear translocation. Therefore, we next investigated for nuclear translocation of β-catenin in insulin-treated ASM and BEAS-2B cells. Increased nuclear localization of β-catenin
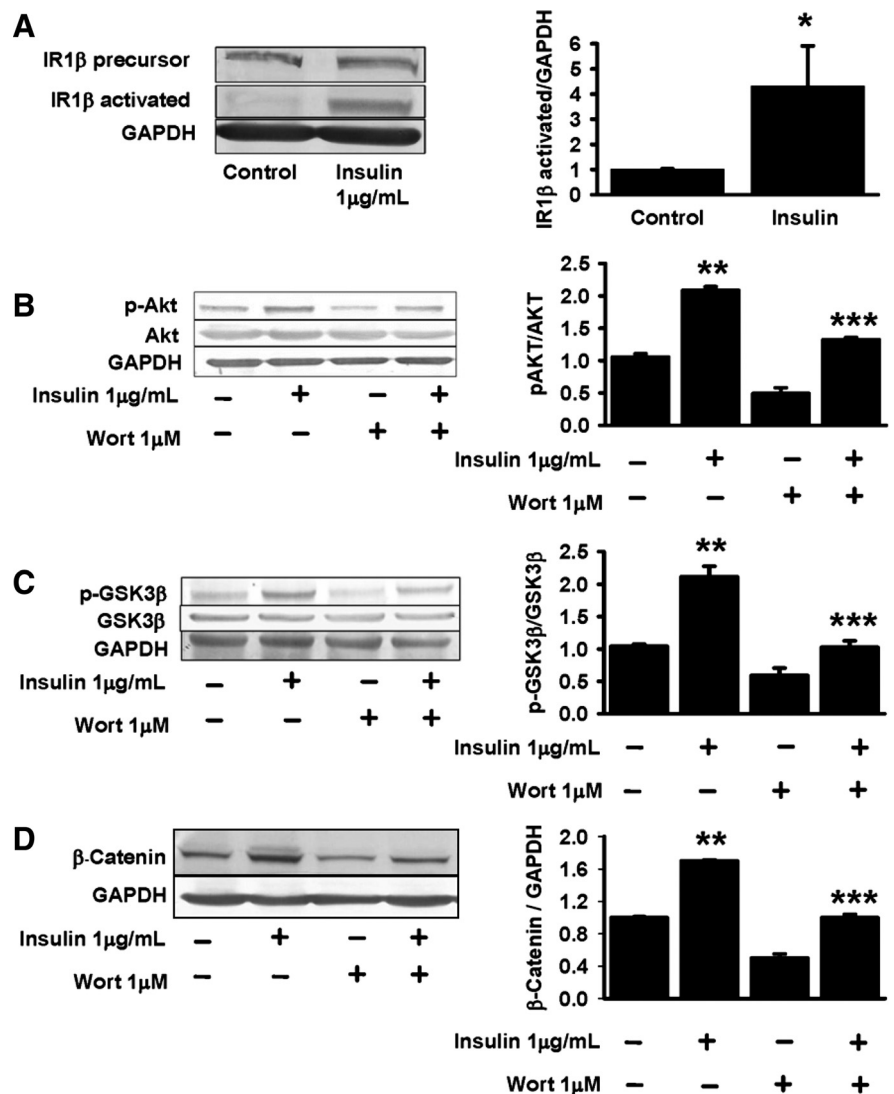

Fig. 4. Insulin enhances β-catenin levels in human lung epithelial cells. The key molecular intermediates of PI3K/Akt signaling have been assessed for their role in insulin-induced increase in β-catenin levels. Human transformed bronchial epithelial (BEAS2B) cells were treated with insulin (1 μg/ml) with/without wortmannin [Wort (1 μM)] pretreatment in vitro. After 24 h the total cell protein was analyzed, by immunoblotting, for activated insulin receptor 1β (IR1β) (*A*), phosphorylated Akt (pAkt; *B*), phosphorylated GSK3β (p-GSK3β; *C*), and β-catenin (*D*). Data represent means ± SE, *n* = 6, *P ≤ 0.05; **P < 0.01 (significant insulin effect); ***P < 0.001 (significant wortmannin effect), compared with wortmannin alone or untreated control. GAPDH, glyceraldehyde-3-phosphate dehydrogenase.

was observed in insulin-treated ASM cells (Fig. 3*A*). Figure 3*B* shows a time-dependent increase in nuclear localization of β-catenin upon insulin treatment in ASM cells. Immunofluorescence imaging for β-catenin in insulin-treated BEAS-2B cells showed an increased colocalization with nucleus compared with untreated controls (Fig. 3, *C* and *D*). The BEAS-2B imaging studies were performed at 24 h and earlier signaling events were dissected through Western blots.

Insulin is known to induce β-catenin through either Wnt signaling or the PI3/Akt pathway, of which the second is part of classical insulin signaling. To determine the role of PI3-Akt-GSK3β activation in insulin-induced β-catenin activation and nuclear translocation, wortmannin, a PI3K inhibitor, was used. Insulin treatment expectedly led to increase in the activated insulin receptor-1β (IR1β), which is known to mediate PI3K activation via insulin receptor substrate (Fig. 4*A*). PI3K inhibition by wortmannin pretreatment reduced phosphorylation of Akt and GSK3β (Fig. 4, *B* and *C*, *left* and *right*). This was associated with significant reduction of the β-catenin levels in both untreated and insulin-treated cells (Fig. 4*D*).

Taken together, these results suggest that insulin induces β-catenin expression in a PI3/Akt pathway-dependent manner.

Insulin Induces a Procontractile and Profibrotic Phenotype in ASM Cells

To understand the importance of the identified insulin-PI3/Akt-β-catenin axis in clinical context, we further investigated the consequences of insulin-treatment on ASM phenotype. First, we confirmed that primary human ASM cells express IR1β (Fig. 5*A*), and insulin treatment to these cells induces phosphorylation of Akt (Fig. 5*B*). Previous studies have shown that insulin induces proliferation of human lung fibroblasts and bovine tracheal smooth muscle cells (15, 40). We found that recombinant human insulin exposure leads to about eightfold increase in human ASM cell number by 72 h (Fig. 5*C*). We further demonstrate that insulin increases $[Ca^{2+}]_i$ levels in human ASM cells (Fig. 5*D*). Both proliferative and contractile ASM phenotypes place metabolic demands on the cells, usually met by mitochondrial oxidative phosphorylation (7, 35).
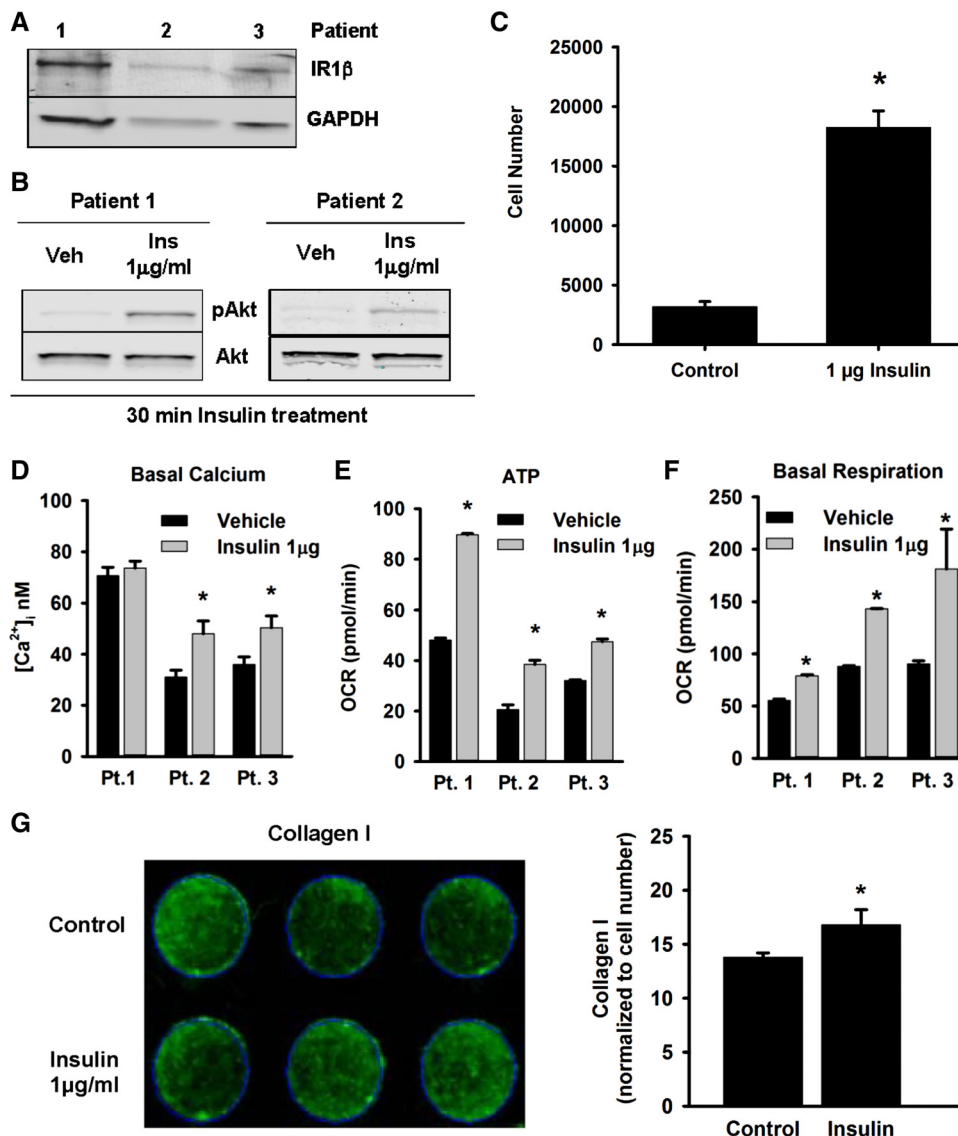

Fig. 5. Insulin induces human airway smooth muscle (ASM) cell proliferation. Insulin-induced phenotypic changes in ASM cells were quantified in primary airway smooth muscle cells isolated from lungs of human donors. Enzymatically dissociated primary human ASM cells, from lung samples of 3 different patients, maintained in culture dishes in vitro were first investigated for the expression of insulin receptor 1β (IR1β) by immunoblotting (*A*). The effect of insulin (1 μg/ml) on human ASM cells was quantified by measuring the following parameters: pAkt levels via immunoblot (*B*), cell proliferation by CellTiter 96 AQueous One Solution Cell Proliferation Assay (*C*), fluorescence-based intracellular basal calcium concentration ($[Ca^{2+}]_i$; *D*), adenosine triphosphate (ATP) (*E*), basal mitochondrial respiration (*F*) by Seahorse Mitochondrial Stress Test, and extracellular collagen-I deposition by a modified in-cell Western blot technique (*G*). The data in *D–G* are represented as mean ± SE of technical replicates for individual patients (Pt.). *$P \leq 0.05$, compared with respective controls. GAPDH, glyceraldehyde-3-phosphate dehydrogenase; Veh, vehicle; Ins, insulin; OCR, oxygen consumption rate.

Induction of ASM cells with insulin led to increases in ATP production and basal mitochondrial respiration in human ASM cells (Fig. 5, *E* and *F*). Interestingly, ASM cells treated with increasing concentrations of insulin demonstrate deposition of collagen-1, a major ECM protein involved in airway remodeling (Fig. 5*G*, *left* and *right*). Overall, these data suggest that insulin can alter human ASM mass and functional phenotype.

DISCUSSION

Previous epidemiological findings have reported associations between low lung function, insulin resistance, and diabetes (6, 14, 38, 41). Inhaled insulin (Exubera, Pfizer) was associated with a decline in forced expiratory volumes in more than half of a small group of patients, before it was withdrawn (5). However, the knowledge of mechanistic underpinnings of these associations is limited and whether insulin may have direct deleterious effects on lung structure or function is not known. The present study importantly fills this gap and finds potential deleterious effects of high levels of insulin on the lung that could help understand the aforementioned epidemiological and clinical observations. Our data provide a partial mechanistic understanding of such effects and implicate activation of the PI3/Akt-β-catenin axis in hyperinsulinemic effects on the lung. β-Catenin activation in primary human airway smooth muscle cells, in an insulin-dependent manner, leads to a proconstrictive and profibrotic phenotype that fits the mixed obstructive as well as restrictive lung function changes in clinical studies of diabetes and inhaled insulin, in relation to respiratory health.

In our experimental studies, mice treated with intranasal insulin showed peribronchial thickening, collagen deposition, and increased AHR. Furthermore, we found that insulin can directly induce molecular signaling events associated with airway smooth muscle proliferation, collagen deposition, and epithelial mesenchymal transition (EMT). A link between insulin resistance, consequent hyperinsulinemia, and asthma is well supported by previous evidence (2, 34, 38). Increased fasting insulin levels are previously reported in humans with features of insulin resistance (12, 27). We have also confirmed that our in vivo insulin model develops signs of early insulin resistance (Fig. 1*D*). Recent work shows a vagally mediated bronchoconstrictor effect of hyperinsulinemia in rats (28), whereas previous work has shown a hypercontractile effect in bovine ASM (32). We report here that insulin induces proliferation and increased respiration in human ASM cells and speculate that insulin-induced increase in ASM mass, with a procontractile and profibrotic phenotype (see Fig. 5), causes airway contraction and thickening (10), culminating in development of asthma-like features. Toward developing a mechanistic understanding of the effects of insulin on the lung, we show that β-catenin signaling is enhanced by insulin in vitro and in vivo. β-Catenin has been previously implicated in cell proliferation and EMT (22, 30). Previous studies have also confirmed the role of β-catenin in ASM cell contraction (18). Interestingly, β-catenin is also known to translocate into the mitochondria and modulate its functions (26), which is interesting in the context of recent work showing the importance of mitochondria in lung health (7). Activation of β-catenin appears to be mediated largely by PI3K/Akt activation and subsequent inhibition of GSK-3β by phosphorylation. This pathway, which is distinct from Wnt-dependent β-catenin activation (13), is also used by TGF-β1 to induce β-catenin activation in ASM and lung fibroblasts (9). It remains to be investigated whether modulation of β-catenin pathway could be a relevant therapeutic strategy to revert insulin-mediated deleterious changes in the human lung. Additional pathways of insulin action also merit future consideration.

Our work has important general implications that should hopefully lead to questioning of many current trends or practices including use of inhaled insulin formulations in diabetes. We have shown that high insulin levels within the physiological range adversely affect lung structure and function. This should discourage blind use of insulin secretagogues and external insulin. Furthermore, it seems likely that restrictive low lung function in apparently healthy populations may relate to hyperinsulinemia. This has never been explicitly tested, and further studies in cross-sectional and birth cohorts are warranted.

DISCLOSURES

No conflicts of interest, financial or otherwise, are declared by the author(s).

AUTHOR CONTRIBUTIONS

S.S., M.B., N.K.B., B.P., A.G., P.K.P., M.A.T., M.F., and U.M. performed experiments; S.S., M.B., N.K.B., B.P., P.K.P., M.A.T., M.F., U.M., B.G., C.M.P., A.L., Y.S.P., and A.A. analyzed data; S.S., M.B., M.A.T., M.F., U.M., R.G., B.G., C.M.P., A.L., Y.S.P., and A.A. interpreted results of experiments; S.S., M.B., B.P., P.K.P., and M.F. prepared figures; S.S., M.B., R.G., Y.S.P., and A.A. drafted manuscript; N.K.B. and A.A. edited and revised manuscript; A.A. conception and design of research; A.A. approved final version of manuscript.

REFERENCES

1. **Abcejo AJ, Sathish V, Smelter DF, Aravamudan B, Thompson MA, Hartman WR, Pabelick CM, Prakash YS.** Brain-derived neurotrophic factor enhances calcium regulatory mechanisms in human airway smooth muscle. *PLoS One* 7: e44343, 2012.
2. **Agrawal A, Mabalirajan U, Ahmad T, Ghosh B.** Emerging interface between metabolic syndrome and asthma. *Am J Respir Cell Mol Biol* 44: 270–275, 2011.
3. **Agrawal A, Sood A, Linneberg A, Ghosh B.** Mechanistic understanding of the effect of obesity on asthma and allergy. *J Allergy (Cairo)* 2013: 598904, 2013.
4. **Ahmad T, Kumar M, Mabalirajan U, Pattnaik B, Aggarwal S, Singh R, Singh S, Mukerji M, Ghosh B, Agrawal A.** Hypoxia response in asthma: differential modulation on inflammation and epithelial injury. *Am J Respir Cell Mol Biol* 47: 1–10, 2012.
5. **Alabraba V, Farnsworth A, Leigh R, Dodson P, Gough SC, Smyth T.** Exubera inhaled insulin in patients with type 1 and type 2 diabetes: the first 12 months. *Diabetes Technol Ther* 11: 427–430, 2009.
6. **Aparna A.** Pulmonary function tests in type 2 diabetics and non-diabetic people—a comparative study. *J Clin Diagn Res* 7: 1606–1608, 2013.
7. **Aravamudan B, Thompson MA, Pabelick CM, Prakash YS.** Mitochondria in lung diseases. *Expert Rev Respir Med* 7: 631–646, 2013.
8. **Assad N, Qualls C, Smith LJ, Arynchyn A, Thyagarajan B, Schuyler M, Jacobs DR Jr, Sood A.** Body mass index is a stronger predictor than the metabolic syndrome for future asthma in women. The longitudinal CARDIA study. *Am J Respir Crit Care Med* 188: 319–326, 2013.
9. **Baarsma HA, Spanjer AI, Haitsma G, Engelbertink LH, Meurs H, Jonker MR, Timens W, Postma DS, Kerstjens HA, Gosens R.** Acti-

vation of WNT/beta-catenin signaling in pulmonary fibroblasts by TGF-beta(1) is increased in chronic obstructive pulmonary disease. *PLoS One* 6: e25450, 2011.

10. **Berair R, Saunders R, Brightling CE.** Origins of increased airway smooth muscle mass in asthma. *BMC Med* 11: 145, 2013.

11. **Beuther DA.** Recent insight into obesity and asthma. *Curr Opin Pulm Med* 16: 64–70, 2010.

12. **Chaour M, Theroux P, Gilfix BM, Campeau L, Lesperance J, Ghitescu M, Gelinas F, Solymoss BC.** 'True' fasting serum insulin level, insulin resistance syndrome and coronary artery disease. *Coron Artery Dis* 8: 683–688, 1997.

13. **Ding VW, Chen RH, McCormick F.** Differential regulation of glycogen synthase kinase 3beta by insulin and Wnt signaling. *J Biol Chem* 275: 32475–32481, 2000.

14. **Engstrom G, Hedblad B, Nilsson P, Wollmer P, Berglund G, Janzon L.** Lung function, insulin resistance and incidence of cardiovascular disease: a longitudinal cohort study. *J Int Med* 253: 574–581, 2003.

15. **Gosens R, Nelemans SA, Hiemstra M, Grootte Bromhaar MM, Meurs H, Zaagsma J.** Insulin induces a hypercontractile airway smooth muscle phenotype. *Eur J Pharmacol* 481: 125–131, 2003.

16. **Guerra S, Sherrill DL, Venker C, Ceccato CM, Halonen M, Martinez FD.** Morbidity and mortality associated with the restrictive spirometric pattern: a longitudinal study. *Thorax* 65: 499–504, 2010.

17. **Husemoen LL, Glumer C, Lau C, Pisinger C, Morch LS, Linneberg A.** Association of obesity and insulin resistance with asthma and aeroallergen sensitization. *Allergy* 63: 575–582, 2008.

18. **Jansen SR, Van Ziel AM, Baarsma HA, Gosens R.** β-Catenin regulates airway smooth muscle contraction. *Am J Physiol Lung Cell Mol Physiol* 299: L204–L214, 2010.

19. **Kent BD, Lane SJ.** Twin epidemics: asthma and obesity. *Int Arch Allergy Immunol* 157: 213–214, 2012.

20. **Kesavadev JD, Short KR, Nair KS.** Diabetes in old age: an emerging epidemic. *J Assoc Physicians India* 51: 1083–1094, 2003.

21. **Kinney GL, Black-Shinn JL, Wan ES, Make B, Regan E, Lutz S, Soler X, Silverman EK, Crapo J, Hokanson JE; COPDGene Investigators.** Pulmonary function reduction in diabetes with and without chronic obstructive pulmonary disease. *Diabetes Care* 37: 389–395, 2014.

22. **Kumawat K, Koopmans T, Gosens R.** β-Catenin as a regulator and therapeutic target for asthmatic airway remodeling. *Expert Opin Ther Targets* 18: 1023–1034, 2014.

23. **Lindberg A, Larsson LG, Ronmark E, Lundback B.** Co-morbidity in mild-to-moderate COPD: comparison to normal and restrictive lung function. *COPD* 8: 421–428, 2011.

24. **Ma J, Xiao L, Knowles SB.** Obesity, insulin resistance and the prevalence of atopy and asthma in US adults. *Allergy* 65: 1455–1463, 2010.

25. **Mannino DM, McBurnie MA, Tan W, Kocabas A, Anto J, Vollmer WM, Buist AS; BOLD Collaborative Research Group.** Restricted spirometry in the Burden of Lung Disease Study. *Int J Tuberc Lung Dis* 16: 1405–1411, 2012.

26. **Mezhybovska M, Yudina Y, Abhyankar A, Sjolander A.** Beta-catenin is involved in alterations in mitochondrial activity in non-transformed intestinal epithelial and colon cancer cells. *Br J Cancer* 101: 1596–1605, 2009.

27. **Modan M, Halkin H, Almog S, Lusky A, Eshkol A, Shefi M, Shitrit A, Fuchs Z.** Hyperinsulinemia. A link between hypertension obesity and glucose intolerance. *J Clin Invest* 75: 809–817, 1985.

28. **Nie Z, Jacoby DB, Fryer AD.** Hyperinsulinemia potentiates airway responsiveness to parasympathetic nerve stimulation in obese rats. *Am J Respir Cell Mol Biol* 51: 251–261, 2014.

29. **Paek YJ, Jung KS, Hwang YI, Lee KS, Lee DR, Lee JU.** Association between low pulmonary function and metabolic risk factors in Korean adults: the Korean National Health and Nutrition Survey. *Metabolism* 59: 1300–1306, 2010.

30. **Pain M, Bermudez O, Lacoste P, Royer PJ, Botturi K, Tissot A, Brouard S, Eickelberg O, Magnan A.** Tissue remodelling in chronic bronchial diseases: from the epithelial to mesenchymal phenotype. *Eur Respir Rev* 23: 118–130, 2014.

31. **Sathish V, Vanoosten SK, Miller BS, Aravamudan B, Thompson MA, Pabelick CM, Vassallo R, Prakash YS.** Brain-derived neurotrophic factor in cigarette smoke-induced airway hyperreactivity. *Am J Respir Cell Mol Biol* 48: 431–438, 2013.

32. **Schaafsma D, McNeill KD, Stelmack GL, Gosens R, Baarsma HA, Dekkers BG, Frohwerk E, Penninks JM, Sharma P, Ens KM, Nelemans SA, Zaagsma J, Halayko AJ, Meurs H.** Insulin increases the expression of contractile phenotypic markers in airway smooth muscle. *Am J Physiol Cell Physiol* 293: C429–C439, 2007.

33. **Shah SH, Sonawane P, Nahar P, Vaidya S, Salvi S.** Pulmonary function tests in type 2 diabetes mellitus and their association with glycemic control and duration of the disease. *Lung India* 30: 108–112, 2013.

34. **Singh S, Prakash YS, Linneberg A, Agrawal A.** Insulin and the lung: connecting asthma and metabolic syndrome. *J Allergy* 2013: 627384, 2013.

35. **Taille C, El-Benna J, Lanone S, Boczkowski J, Motterlini R.** Mitochondrial respiratory chain and NAD(P)H oxidase are targets for the antiproliferative effect of carbon monoxide in human airway smooth muscle. *J Biol Chem* 280: 25350–25360, 2005.

36. **Tesse R, Schieck M, Kabesch M.** Asthma and endocrine disorders: shared mechanisms and genetic pleiotropy. *Mol Cell Endocrinol* 333: 103–111, 2011.

37. **Thomsen SF, Duffy DL, Kyvik KO, Skytthe A, Backer V.** Risk of asthma in adult twins with type 2 diabetes and increased body mass index. *Allergy* 66: 562–568, 2011.

38. **Thuesen BH, Husemoen LL, Hersoug LG, Pisinger C, Linneberg A.** Insulin resistance as a predictor of incident asthma-like symptoms in adults. *Clin Exp Allergy* 39: 700–707, 2009.

39. **Wan ES, Hokanson JE, Murphy JR, Regan EA, Make BJ, Lynch DA, Crapo JD, Silverman EK.** Clinical and radiographic predictors of GOLD-unclassified smokers in the COPDGene study. *Am J Respir Crit Care Med* 184: 57–63, 2011.

40. **Warnken M, Reitzenstein U, Sommer A, Fuhrmann M, Mayer P, Enzmann H, Juergens UR, Racke K.** Characterization of proliferative effects of insulin, insulin analogues and insulin-like growth factor-1 (IGF-1) in human lung fibroblasts. *Naunyn Schmiedeberg's Arch Pharmacol* 382: 511–524, 2010.

41. **Young RP, Hopkins R, Eaton TE.** Forced expiratory volume in one second: not just a lung function test but a marker of premature death from all causes. *Eur Respir J* 30: 616–622, 2007.